JOURNAL OF CATALYSIS **161,** 338–349 (1996)
ARTICLE NO. 0191

Dealumination of HZSM-5 Zeolites

I. Calcination and Hydrothermal Treatment[1]

Sharelle M. Campbell,*,† David M. Bibby,‡ Jan M. Coddington,† Russell F. Howe,§,[2] and Richard H. Meinhold‡

*Chemistry Department, Louisiana State University, Shreveport, Louisiana 71105; ‡Industrial Research Ltd, Petone, New Zealand; †Chemistry Department, University of Auckland, Auckland, New Zealand; and §Department of Physical Chemistry, University of New South Wales, Australia

Received August 21, 1995; revised November 28, 1995; accepted January 31, 1996

The effect of calcination and hydrothermal treatments on the structure and properties of HZSM-5 zeolites with a range of aluminum contents has been investigated. Characterization of the treated zeolites was undertaken with solid-state NMR (^{27}Al and ^{29}Si), infrared, nitrogen and water adsorption, X-ray diffraction, X-ray photoelectron spectroscopy, scanning electron microscopy, chemical analysis, and ^{129}Xe NMR spectroscopy. Both calcination and hydrothermal treatment were found to cause dealumination of the zeolite lattice and formation of extralattice aluminum species of low symmetry which remain within the pores of the zeolite. HZSM-5 with low aluminum content was found to be more resistant to dealumination by either method and the degree of dealumination was greater when steam was present in the treatment. ^{129}Xe NMR was found to be a useful probe for the presence of extralattice aluminum in the pores of lattice dealuminated HZSM-5.

INTRODUCTION

The acid properties and resultant catalytic activity of zeolite materials are known to be related to the degree of substitution of aluminum for silicon in the framework. The modification of catalytic properties through dealumination of zeolite lattices by various treatments has therefore been a matter of considerable interest. ZSM-5 is known to be more resistant to dealumination than Y or mordenite zeolites (1), but nonetheless dealumination of the lattice does occur (2–4) when the zeolite is subjected to steam at high temperatures.

A number of studies are reported in the literature which deal with individual facets of dealumination of the HZSM-5 zeolite lattice following various treatments (2–10). These studies have employed solid-state NMR spectroscopy and/or infrared spectroscopy.

Fyfe *et al.* (5) have shown that ^{29}Si NMR spectra of ZSM-5 contain signals due to Si(1Al) and Si(0Al). Upon dealumination, the signal due to Si(1Al) decreases and becomes unobservable when the Si/Al ratio of the framework is greater than 125 (2). As the aluminum content decreases further, the Si(0Al) signal narrows and, when spectra are recorded at high field, crystallographically distinct Si(0Al) sites can be resolved.

The ^{27}Al NMR signal due to tetrahedral lattice aluminum appears at ca. 54–56 ppm for hydrated HZSM-5 zeolites. Loss of the total aluminum signal following treatment has been widely reported (2–4) and attributed to dealumination of the zeolite lattice. However, a signal of small intensity appears at 0 ppm following dealumination. In addition, a broad peak with a maximum at 30–40 ppm has been observed (6, 7) in high field ^{27}Al NMR spectra of hydrothermally dealuminated ZSM-5. This resonance has been attributed to highly distorted, tetrahedral, nonframework, aluminum–oxygen species (8), although the chemical shift is also consistent with 5-coordinate aluminum (11).

HZSM-5 contains only one kind of bridging hydroxyl group, with a stretching frequency of 3610 cm^{-1} (12). Lago and co-workers (10) have shown in studies of untreated HZSM-5 that the intensity of the band is proportional to the aluminum content of the lattice as measured by ^{27}Al NMR. A band appearing at 3660 cm^{-1} following hydrothermal treatment was noted and assigned to hydroxyls associated with extra framework aluminum. This band has also been described more recently by Maijanen *et al.* (9).

A number of researchers (13–15) have observed that the degree of lattice dealumination of faujasite zeolites following steam treatment is dependent on the temperature at which the treatment is carried out; higher temperatures lead to a higher degree of dealumination.

[1] This work is dedicated to the memory of Dr. Jan M. Coddington, one of the authors of the paper, who died tragically in May 1992.

[2] To whom correspondence should be addressed at the Department of Physical Chemistry, University of New South Wales, Sydney NSW 2052, Australia.

0021-9517/96 $18.00

TABLE 1

Characteristics of the Zeolite Samples

Sample	Z12	Z20	Z25	Z74	Z94	Z121
Si/Al[a]	11.7	20.2	24.9	74	94	121
Al/uc	7.59	4.53	3.71	1.28	1.01	0.79
Preparation method	Inorg.[b]	Inorg.[b]	Inorg.[b]	TPA[c]	TPA[c]	TPA[c]
Form as received	Na	Na	Na	H	TPA	TPA
Pretreatment	NH_4 exch.	NH_4 exch.	NH_4 exch.	None	Calcin.[d] NH_4 exch.	Calcin.[d] NH_4 exch.
Crystal morphology	Ellip.	Flakes, irreg.	Irreg.	Sphere	Cube	Lath
Crystal size	<1 μm	<1 μm	<1 μm	<1 μm diameter	35 μm	4 μm long

[a] From chemical analysis.
[b] Commercial sample.
[c] Prepared at Department of Scientific and Industrial Research, Petone, NZ, by the Argauer and Landbolt method.
[d] Calcination at 873 K in dry flowing air for 24 h to remove tetrapropyl ammonium (TPA) template.

Few studies of the effects of treatment variables on the dealumination of ZSM-5 have been reported in the literature. Brunner *et al.* (7) investigated the effect of a mild hydrothermal treatment on the aluminum contained in HZSM-5 as a function of water vapor pressure. The degree of dealumination was shown in this study to be strongly dependent upon the water vapor pressure at pressures below 20 kPa, and relatively constant at higher pressures. Maijanen *et al.* recently described a study by FTIR and solid-state NMR of the progressive dealumination of a ZSM-5 zeolite as a function of exposure to steam at 350°C (9). That study showed that the number of Brønsted acid sites decreased progressively as the steaming time increased. Evidence was also presented for formation of weakly acidic AlOH groups and SiOH defects at intermediate steaming times.

In an effort to develop a more systematic understanding of HZSM-5 lattice dealumination and the structure of the dealuminated samples, we present here measurements of lattice aluminum contents, hydroxyl group and acid site concentrations in HZSM-5 before and after hydrothermal treatment for samples of HZSM-5 of varying aluminum contents. We wished in particular to investigate the importance of the lattice aluminum content as a variable in the dealumination chemistry. The dealumination of the zeolite lattice and the nature and location of extralattice aluminum following these treatments involving calcination and hydrothermal treatments of increasing severity were studied using a range of experimental techniques. This work was undertaken as a necessary prerequisite to studies of dealumination during the methanol to gasoline reaction, described in the accompanying paper.

EXPERIMENTAL

Calcination and Hydrothermal Treatment

Six samples of ZSM-5 differing in aluminum content (Table 1) as determined by atomic absorption spectroscopy, were used in this study. HZSM-5 was prepared by ammonium ion exchange and subsequent deammonation of the NH_4ZSM-5 by calcining, as described below. The use of dry flowing nitrogen and slow heating ensured minimal dealumination of the zeolite lattice during this step, as can be seen from the data in Table 2.

Hydrothermal treatment of 0.5-g samples was carried out in a quartz reactor tube with 10 mm maximum bed depth of zeolite. The temperature was increased at a rate of 5 K min^{-1} to treatment temperature under a dry nitrogen flow of 100 ml min^{-1}. Steam treatment was carried out at various temperatures and for various times (Table 2), under a water vapor pressure of ca. 15 Torr generated by diversion of the nitrogen gas stream through a water bubbler at room temperature.

The zeolite samples were calcined in the same quartz reactor and in a similar manner to the hydrothermal treatments. A flow of dry nitrogen (100 ml min^{-1}) through the sample bed was maintained during calcination. Details of the treatments are given in Table 2.

Extraction of extralattice aluminum from a sample of hydrothermally treated HZSM-5 was carried out using an

TABLE 2

Treatment of HZSM-5 Zeolite Samples

Treatment nomenclature	Treatment details			
	Pretreatment	Temperature (K)	Duration (h)	Treatment gas
HD	Deammonation	998	7	Dry N_2
LS	Deammonation	873	1.5	H_2O in N_2
HS	Deammonation	1023	7	H_2O in N_2
VHS	Deammonation	1113	24	H_2O in N_2

Note. NH, zeolite left in original ammonium form or deammoniated *in situ* during measurement. H, (deammonated) heated over 1 h to 373 K, held 1 h, heated over 2 h to 673 K, held 4 h in dry flowing N_2.

aqueous solution of hexafluorosilicate at 333 K over 3 h. The concentration of the ammonium hexafluorosilicate solution (SiF_6^{2-}) used for extraction was such that there was a one to one ratio between the number of moles of SiF_6^{2-} in the washing solution and the number of moles of extralattice aluminum expected to be present in the zeolite sample. The extracted sample was washed three times with deionized water at 333 K to remove any traces of extracting solution and then dried at 363 K.

NMR Measurements

^{29}Si and ^{27}Al MAS NMR measurements were carried out on rehydrated samples, which had been kept in a desiccator over saturated aqueous NH_4Cl (80% relative humidity), for 7 days. The NMR spectra, both ^{27}Al and ^{29}Si, were recorded on a Varian XL200 spectrometer. At the magnetic field of 4.7 T, the frequencies of ^{27}Al and ^{29}Si are 52.128 and 39.7455 MHz, respectively.

For the recording of ^{27}Al spectra, a spectral width of 50 kHz, an acquisition time of 0.02 s, and a delay between pulses of 0.1 s were used. A pulse length of 1.0 ms ($\pi/12$) was used to ensure uniform excitation of both low and high electric field gradient nuclei for quantitative work. The reference used for these studies was the octahedral signal of the hydrated Al^{3+} cation in solid aluminum chloride hexahydrate.

^{29}Si NMR spectra were recorded with a spectral width of 10 kHz, an acquisition time of 0.02 s, and delays between pulses of 12 s. A 90° pulse of 6 ms was used to acquire the ^{29}Si Bloch decays. High power proton decoupling ($-B/2\pi \sim 60$ kHz) was applied during acquisition for both ^{27}Al and ^{29}Si NMR. The ^{29}Si NMR signal of TMS was used as the chemical shift reference in these studies. For ^{29}Si cross-polarization a recycle time of 0.1 s and a contact time of 5000 ms were used. Free induction decays were zero filled to 8 k and Fourier transformed after 50 Hz (for Al) or 20 Hz (for Si) Lorentzian line broadening.

Acetylacetone was adsorbed onto treated HZSM-5 samples and the ^{27}Al MAS NMR measurements were repeated in an effort to render "NMR visible" both lattice and extralattice aluminum. The HZSM-5 samples were dried in an oven at 433 K to remove adsorbed water. After being held at this temperature for 24 h, the samples were transferred to a desiccator containing acetylacetone. The desiccator was evacuated and the samples left to cool and equilibrate for 5 days at room temperature. The samples were removed from the evacuated desiccator and the NMR spectra recorded within a few hours in order to minimize loss of adsorbed acetylacetone from the zeolite samples (16).

FTIR Measurements

The *in situ* infrared experiments were carried out in a controlled atmosphere cell similar to that described by Katzer *et al.* (17). Zeolite samples were pressed into self-supporting wafers (5–20 mg cm^{-2}), mounted in the cell and activated by heating in flowing dry nitrogen to 673 K. For measurement of the hydroxyl vibrations, spectra were recorded following cooling of the wafer to 423 K.

Pyridine (10 ml) was injected by syringe through a septum into the gas flow. To increase the contact time of the pyridine on the zeolite wafer the nitrogen flow rate was reduced to 80 ml min^{-1} for 2 min at the time of injection. Spectra were recorded at 423 K after 10 min flushing of the cell at 200 ml min^{-1} in order to reduce the contribution to spectra of gas phase and physisorbed pyridine.

Infrared spectra were recorded on a Nicolet 5DX FTIR spectrometer at a resolution of 4 cm^{-1} and typically 200 interferograms were averaged. Subtraction of the spectra taken prior to adsorption yielded difference spectra of the adsorbed species.

Adsorption of gaseous ammonia was carried out by introduction of ammonia to the N_2 gas flowing through the *in situ* IR cell. Infrared spectra were recorded at 423 K and the total acid site concentration was calculated from the area of the absorption band due to adsorbed ammonia.

The framework tetrahedra vibrational stretching modes of zeolites were measured with zeolites diluted with potassium bromide (KBr).

When the zeolite crystal size was >5 μm, preparation of self-supporting wafers became impossible. Thus, for the Z94 HZSM-5 samples, infrared spectra were recorded using diffuse reflectance infrared spectroscopy. The DRIFT accessory used in this study was a Barnes analytical diffuse reflectance unit (model 0030-001) fitted with a controlled atmosphere heated cell.

Measurement of Adsorption Isotherms

Measurement of nitrogen adsorption isotherms was carried out at 77 K after the zeolite samples (~0.15 g) had been outgassed overnight at 648 K, using a Micromeritics Accusorb 2100E instrument. The pore volume was taken from the volume of nitrogen (at STP) adsorbed at $P/P_s = 0.20$.

X-Ray Photoelectron Spectroscopy

XPS measurements were carried out on a Kratos XSAM-800, using a magnesium anode and a pass energy of 65 eV. Pressed pellets of the zeolite were mounted on stainless steel stubs using double-sided Sellotape and degassed for 3–4 h in the preparation chamber. A single narrow scan of the binding energies from 110 to 70 eV recorded both the Si 2p and the Al 2p peaks and quantitation calculations were performed using Kratos software.

^{129}Xe NMR Measurements

^{129}Xe NMR spectra were recorded as outlined in Ref. 18. Prior to xenon adsorption all adsorbed water and any residual ammonium ions were removed by degassing ca. 0.15 g of

zeolite at 673 K under vacuum in an NMR tube fitted with a high vacuum stopcock. The quantity of xenon introduced at room temperature into the NMR tube was determined from the increase in mass and a plot of ^{129}Xe chemical shift as a function of xenon concentration was prepared. The amounts of adsorbed xenon were determined from xenon adsorption isotherms measured separately.

RESULTS

Chemical Analysis

For none of the treated and unextracted samples was any loss of bulk aluminum from the zeolite noted. Within the ± 5% experimental error of the analysis the Si/Al ratio remained the same, in all cases. However, chemical analysis of the extracted sample (Z20S/SW) indicated that the ammonium hexafluorosilicate extraction had removed 70% of the total aluminum from the zeolite. Scanning electron micrographs of the treated samples showed no observable differences in morphology, while the X-ray powder diffraction patterns indicated no observable reduction in crystallinity.

Solid-State NMR Spectroscopy

Figure 1 shows the ^{27}Al MAS NMR spectra of the hydrated Z12 HZSM-5 zeolites. Upon deammonation of the zeolite, the peak area of the signal at 53 ppm, due to tetrahedral aluminum was reduced and a signal appeared at −2 ppm. On calcination or hydrothermal treatment, the tetrahedral aluminum, signal decreased further and the intensity of the signal at −2 ppm assigned to octahedral aluminum remained the same or decreased. Using peak area measurement with correction for sample mass, number of scans, and plotting scales, the aluminum in tetrahedral lattice positions and octahedral aluminum species were quantified and, from the known bulk aluminum content of the zeolite, the "NMR invisible" extralattice aluminum content was calculated. Results of these measurements for the treated zeolites with different Si/Al ratios are given in Table 3.

The sample of hydrothermally treated HZSM-5 which had been washed with hexafluorosilicate showed no loss of ^{27}Al NMR signal attributed to tetrahedral lattice aluminum when compared to the sample prior to extraction, but complete loss of the small signal attributed to octahedral extralattice aluminum.

Figure 2 shows the ^{27}Al MAS NMR spectra of the HZSM-5 samples, onto which acetylacetone had been adsorbed following the calcination or hydrothermal treatment. There are several differences noted in the spectra following adsorption of acetylacetone. In particular the intensity of the tetrahedral ^{27}Al NMR signal decreases, the chemical shift of this signal is also reduced by about 3 ppm, and a new signal appears at a chemical shift characteristic of octahedral aluminum (ca. 1 ppm).

As the ^{27}Al NMR signal attributed to tetrahedral lattice aluminum decreased on calcination or hydrothermal treatment, the intensity of the octahedral aluminum signal following acetylacetone adsorption increased. The ^{27}Al NMR spectrum of the Z20S/SW sample did not show the sharp

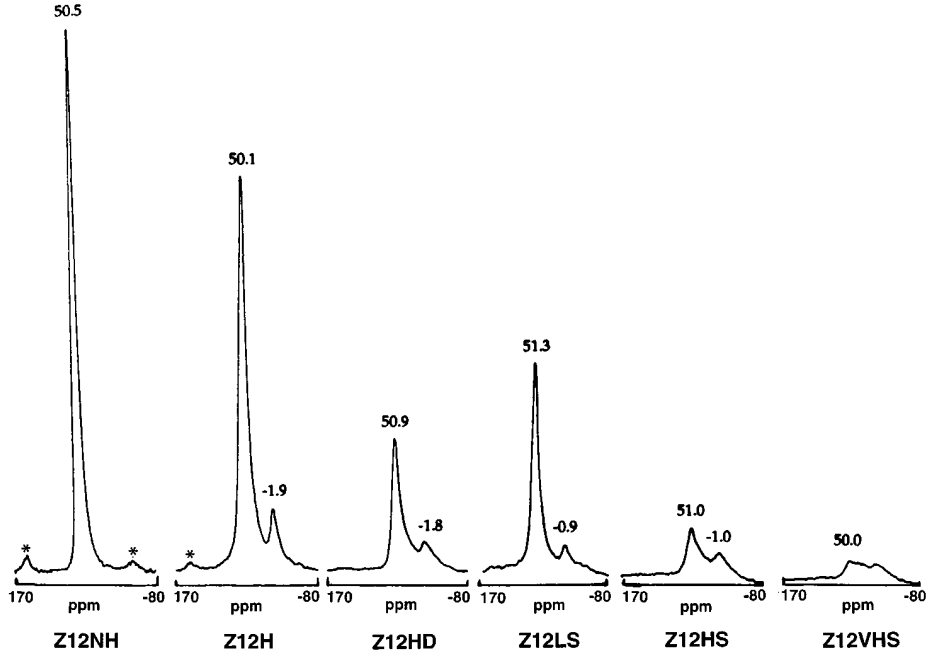

FIG. 1. ^{27}Al MAS NMR spectra of HZSM-5 after various treatments. * Spinning side bands.

TABLE 3

Characterization of Calcined and Hydrothermally Treated HZSM-5 Samples

Sample	Lattice Al (NMR) ($Al(uc)^{-1}$)	Extralattice Al (NMR) ($Al(uc)^{-1}$)	Octahedral content (^{27}Al NMR) ($Al(uc)^{-1}$, ±20%)	Bridging hydroxyl conc. (IR) ($(uc)^{-1}$, ±10%)	Brønsted acid conc. (py. ads.) ($(uc)^{-1}$, ±5%)	Lewis acid conc. (py. ads.) ($(uc)^{-1}$, ±5%)	Lattice Al content (framework IR) ($Al(uc)^{-1}$, ±1.0%)	Pore volume (from N_2 isotherm) ($cm^3\ g^{-1}$, ±3%)	Chemical shift extrapolated to zero xenon (ppm, ±1.5)	Lattice Al content (^{129}Xe NMR) ($Al(uc)^{-1}$, ±1.0)
Z12NH	7.6 ± 0.1	—	0.0	7.6	7.5	0.1	—	—	—	—
Z12H	7.2 ± 0.5	0.4 ± 0.6	0.4	6.9	7.3	0.5	7.5	104.4	113.5	7.5
Z12HD	2.5 ± 0.3	5.1 ± 0.4	0.4	2.2	2.4	1.0	3.7	94.6	110.9	4.3
Z12LS	3.6 ± 0.4	4.0 ± 0.5	0.2	3.5	5.0	0.8	3.8	97.6	112.8	6.4
Z12HS	1.2 ± 0.2	6.4 ± 0.3	0.3	—	1.3	0.9	1.9	92.6	109.6	4.0
Z12VHS	0.2 ± 0.2	7.4 ± 0.3	0.4	—	0.6	0.3	0.2	92.6	105.1	1.8
Z20H	4.3 ± 0.2	0.2 ± 0.2	0.0	4.4	4.1	0.4	4.5	91.4	111.1	4.5
Z20HD	3.1 ± 0.4	1.4 ± 0.6	0.2	1.8	3.1	0.7	3.0	89.1	107.2	3.2
Z20LS	3.2 ± 0.4	1.3 ± 0.6	0.2	3.5	3.2	0.4	3.6	90.3	108.4	3.5
Z20HS	0.6 ± 0.2	3.9 ± 0.4	0.2	0.7	0.8	0.5	1.7	86.5	106.8	2.5
Z20S	0.6 ± 0.2	3.9 ± 0.4	0.2	0.6	0.8	1.4	0.6	82.3	106.2	2.0
Z20S/SW	0.6 ± 0.2	0.6 ± 0.4	0.0	0.6	0.7	0.3	0.6	88.0	—	—
Z25NH	3.7 ± 0.1	—	0.0	3.7	3.5	0.2	—	—	—	—
Z25H	3.5 ± 0.3	0.2 ± 0.4	0.1	3.2	3.8	0.4	3.7	90.3	109.5	3.7
Z25HD	2.0 ± 0.3	1.7 ± 0.4	0.1	2.1	2.5	0.4	2.6	87.8	105.6	1.8
Z25LS	1.9 ± 0.3	1.8 ± 0.4	0.1	1.7	2.7	0.4	2.9	90.6	107.1	2.5
Z25HS	0.5 ± 0.2	3.2 ± 0.3	0.1	0.5	0.9	0.6	1.7	82.0	104.4	1.2
Z74H	1.2 ± 0.1	0.1 ± 0.1	0.04	1.2	1.17	0.13	1.2	117.1	103.2	0.7
Z74DH	1.1 ± 0.1	0.1 ± 0.2	0.03	1.1	1.09	0.29	1.1	117.6	103.7	0.9
Z74LS	1.0 ± 0.1	0.2 ± 0.2	0.00	1.0	1.00	0.21	1.1	118.5	102.3	0.4
Z74HS	0.8 ± 0.1	0.4 ± 0.2	0.00	0.8	0.85	0.21	0.9	114.1	101.9	0.1
Z94NH	1.01 ± 0.05	—	0.00	—[a]	—[a]	—[a]	—	—	—	—
Z94H	0.93 ± 0.09	0.1 ± 0.1	0.03	—[a]	—[a]	—[a]	—[b]	114.7	102.6	0.5
Z94HD	0.85 ± 0.09	0.2 ± 0.1	0.00	—[a]	—[a]	—[a]	—[b]	118.8[c]	105.1	1.3
Z94LS	0.79 ± 0.09	0.2 ± 0.1	0.00	—[a]	—[a]	—[a]	—[b]	122.4[c]	105.0	1.3
Z94HS	0.58 ± 0.08	0.4 ± 0.1	0.01	—[a]	—[a]	—[a]	—[b]	114.7	101.3	0.2
Z121NH	0.77 ± 0.05	—	0.00	0.77	0.79	0.08	—	—	—	—
Z121H	0.79 ± 0.05	0.0 ± 0.1	0.00	0.79	0.78	0.08	0.8	99.0	103.4	0.9
Z121HD	0.66 ± 0.07	0.1 ± 0.1	0.00	0.68	0.70	0.08	0.8	98.6	104.1	1.0
Z121LS	0.67 ± 0.07	0.2 ± 0.1	0.00	0.66	0.62	0.10	0.8	99.0	102.9	0.7
Z121HS	0.59 ± 0.07	0.3 ± 0.1	0.00	0.56	0.60	0.20	0.8	96.2	102.2	0.5

[a] Use of diffuse reflectance infrared allows only qualitative information to be obtained for these samples.
[b] Framework vibrational bands distorted due to large crystal size of this sample.
[c] Anomalous step in isotherm at $P/P_0 = 0.05$ yields high values of "pore volume" for these samples.

octahedral peak characteristic of acetylacetone adsorbed on extralattice aluminum (16) which appeared in the spectrum of Z20S.

The ^{29}Si MAS NMR spectra of the Z12 HZSM-5 series are presented in Fig. 3. Heat or hydrothermal treatment caused a marked decrease in intensity of the signal at −105 ppm, attributed to Si(1Al) (13), In the spectrum of Z12VHS, for example, this signal was barely distinguishable. At the same time the remaining signal at −112 ppm due to Si(0Al) narrowed and showed partial resolution of shoulders at higher chemical shift. The ^{29}Si NMR spectra of the Z20S and Z20S/SW HZSM-5 samples were indistinguishable. Because of the complex overlapping nature of signals in the ^{29}Si spectra, quantitative analysis of the Si(1Al) signal intensity was not attempted.

The relative intensities within cross-polarized spectra, of the signals due to silanol groups and tetrahedral Si(0Al) were the same following calcination or hydrothermal treatment; no increase in the proportion of silanol groups was observed following treatment.

Infrared Spectroscopy

The infrared spectra recorded at 423 K of the Z12 series of treated samples, showing the hydroxyl stretching vibration region, are given in Fig. 4. On heat or steam treatment the intense band at 3606 cm^{-1} was progressively lost. Mild treatment produced a new broad hydroxyl band at about 3660 cm^{-1}, but the most severe steam treatment caused the complete removal of both this band and the one at

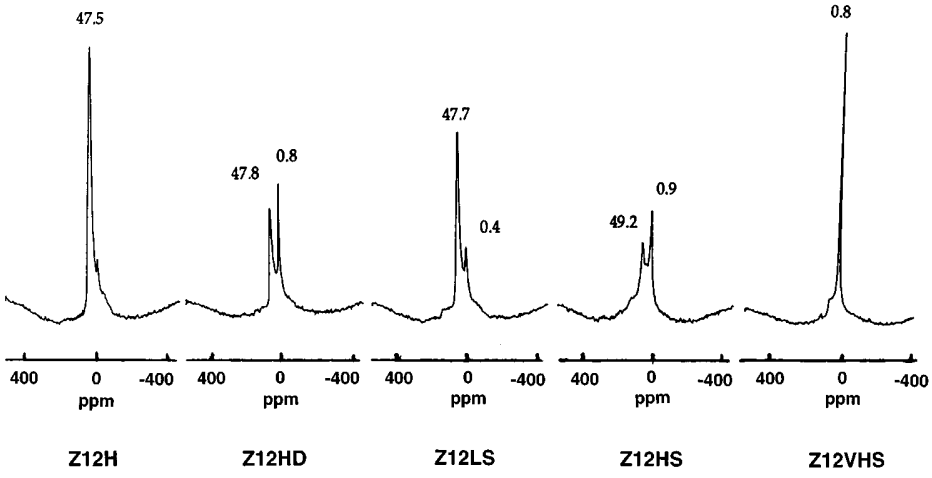

FIG. 2. ^{27}Al MAS NMR spectra of treated HZSM-5 following adsorption of acetylacetone.

3660 cm^{-1}. The third hydroxyl band at 3720 cm^{-1} was only slightly affected by steam treatment.

Quantification of the bridging hydroxyl concentration was carried out by measurement of peak area of the band at 3606 cm^{-1}. Correction for wafer thickness was made from peak areas of the framework overtone bands between 1400 and 2300 cm^{-1}. The bridging hydroxyl concentrations shown in Table 3 were calculated assuming that the hydroxyl concentrations in the parent zeolites were equal to the lattice aluminum contents.

Following adsorption of pyridine, the infrared band at 3606 cm^{-1} was lost and bands due to adsorbed pyridine appeared in the region from 1300 to 1700 cm^{-1}. The bands at 3720 and 3660 cm^{-1}, due respectively to nonacidic silanol groups and hydroxyl groups on extralattice aluminum, remained unperturbed by adsorption of bases. Infrared

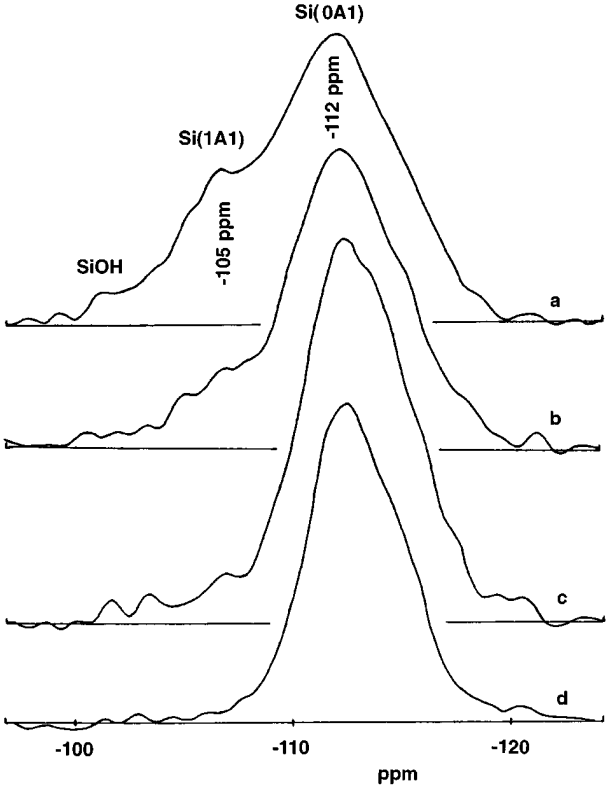

FIG. 3. ^{29}Si MAS NMR spectra of (a) Z12NH, (b) Z12LS, (c) Z12HS, (d) Z12VHS.

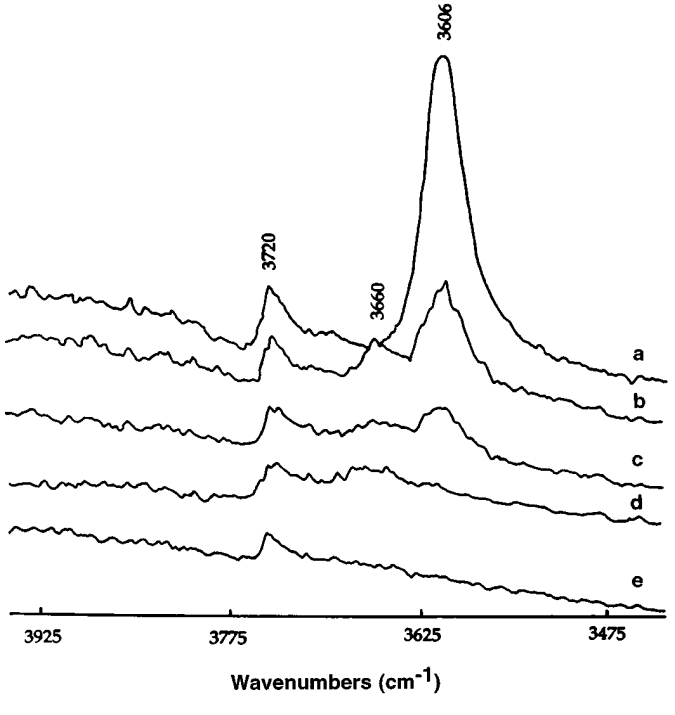

FIG. 4. FTIR spectra of treated HZSM-5: (a) Z12H, (b) Z12LS, (c) Z12HD, (d) Z12HS, (e) Z12VHS.

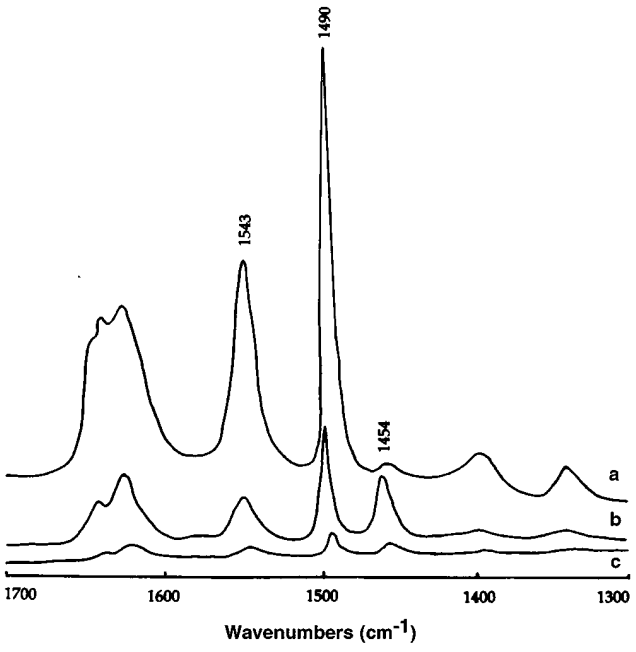

FIG. 5. FTIR spectra of pyridine adsorbed on treated HZSM-5: (a) Z12NH, (b) Z12HS, (c) Z12VHS.

spectra of pyridine adsorbed on treated Z12 HZSM-5 samples are shown in Fig. 5. The spectra shown have been corrected for variations in wafer thickness. The bands at 1543 and 1454 cm^{-1} are assigned to pyridine adsorbed onto Brønsted or Lewis acid sites, respectively, and the Brønsted and Lewis acid site concentrations of each zeolite sample in each of the treated series (Table 3) was determined by measurement of the peak areas of these bands.Correction for differences in absorptivity values (19) were applied and it was assumed that the total acid site concentration of the parent HZSM-5 sample prepared *in situ* was equal to the aluminum content of that zeolite. The hydroxyl regions of the infrared spectra for the Z20S and Z20S/SW HZSM-5 samples were very similar. No loss of intensity of the absorption band at 3606 cm^{-1} was observed following the extraction. Differences in the infrared spectra of adsorbed pyridine were evident, however. The Brønsted acid site concentration was not affected by extraction of the extralattice aluminum but the Lewis acid site concentration decreased markedly.

As a comparison, infrared studies of adsorbed ammonia were also carried out on samples of the Z12 series. A broad absorption band at 1450 cm^{-1} in the infrared spectra can be attributed to ammonia adsorbed on both Brønsted and Lewis acid sites. The total acid site concentration of the treated samples calculated from infrared studies of samples with adsorbed ammonia were found to be the same within experimental error as the total acid site concentrations calculated from pyridine adsorption studies, confirming the data in Table 3.

Infrared spectra of the zeolite lattice vibrational modes observed between 400 and 1300 cm^{-1} were recorded. The absorption bands at ca. 791 and 1087 cm^{-1} are due to the T-O-T asymmetric and symmetric stretching vibrations of the aluminosilicate lattice, respectively (20). The absorption bands at ca. 544 and 1219 cm^{-1} are vibrations associated with the structural assembly of the tetrahedra in HZSM-5 (20). A small shift in the frequency of these absorption bands to lower frequency was observed with decreasing aluminum content for the parent HZSM-5 samples. A similar frequency shift was also observed following calcination or hydrothermal treatment of any particular parent HZSM-5. The wavenumbers of one of the structure sensitive modes (544 cm^{-1}) and one of the general aluminosilicate vibrations (791 cm^{-1}) are shown plotted as a function of HZSM-5 lattice aluminum content in Fig. 6. The framework vibration bands also became narrower for samples treated above 873 K.

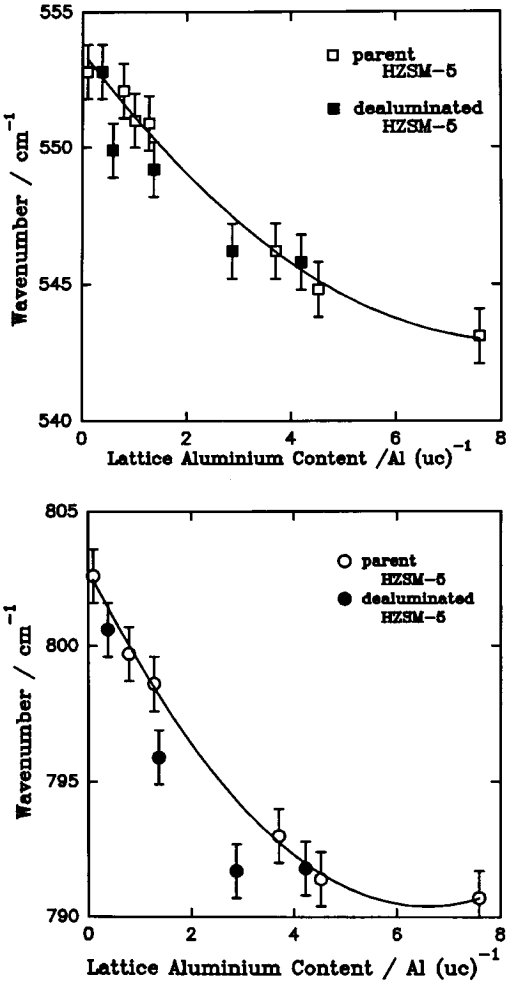

FIG. 6. Framework vibration frequencies as a function of the lattice aluminum content for the 554 and 790 cm^{-1} infrared absorption bands.

Nitrogen Adsorption Isotherms

The adsorption isotherms of nitrogen measured at 77 K were recorded for both parent and treated HZSM-5. Treatment of the zeolite led to a loss in the volume of nitrogen adsorbed, but no change in the appearance of the isotherm. In this work the value quoted as the pore volume of the zeolite is the volume at STP of nitrogen adsorbed in the zeolite at $P/P_0 = 0.2$. An error of $\pm 3\%$ in the pore volume was estimated from repeated measurement on the same zeolite sample. The values of pore volume are listed in Table 3.

Thermogravimetric Analysis of Adsorbed Water

Water contents of the HZSM-5 samples, both parent and treated, were determined by thermogravimetric analysis. It was found that the mass of water adsorbed in the parent HZSM-5 samples can be correlated with the aluminum content of the zeolite. The water content of the zeolite is expressed as the weight of water adsorbed at equilibrium, at a relative humidity of 80%, per gram of dry zeolite. The water content of the parent HZSM-5 samples is plotted as a function of the total aluminum content of the zeolite in Fig. 7. Also shown in Fig. 7 is the water content of the calcined and hydrothermally treated zeolites, as a function of the lattice aluminum content calculated from ^{27}Al NMR spectra. The mass of water adsorbed was greater in all cases for the dealuminated zeolites containing extralattice aluminum than that expected for an untreated HZSM-5 of the same lattice aluminum content. Following extraction of 85% of the extralattice aluminum from the Z20S hydrothermally treated HZSM-5 (Z20S/SW), the water content fell on the same curve as HZSM-5 samples containing no extralattice aluminum.

X-Ray Photoelectron Spectroscopy

The sample Z12H had a surface Si/Al ratio of 14.0 ± 1.5 as compared to a bulk Si/Al ratio of 11.7. Surface depletion of aluminum in zeolites as prepared has been reported previously in the literature (21). Surface Si/Al ratios of treated Z12 HZSM-5 samples ranged from 10.9 to 12.5, i.e., the aluminum content at the surface increased slightly following treatment. The uncertainty in Si/Al ratio was due to the relatively low intensity of the Al 2p peak and for the same reason it was not possible to study zeolites of Si/Al ratio greater than 25 by XPS.

^{129}Xe NMR Spectroscopy

Xenon adsorbed in all of the zeolites studied gave a single ^{129}Xe NMR signal. The chemical shift of the signal was determined as a function of either the xenon introduced into the sample tube or as a function of the xenon adsorbed on the zeolite depending on the information required. The chemical shift as a function of xenon adsorbed in the zeolite for the Z12 treated samples is shown in Fig. 8. The initial gradients of these curves were the same within experimental error.

The values of chemical shift extrapolated to zero xenon coverage measured for the treated HZSM-5 samples are given in Table 3. These values were determined from intercepts of the plots of chemical shift as a function of xenon introduced into the NMR tube. The intercept value decreased as a result of treatment of the zeolite. We have shown previously (18) that there is a relationship between the aluminum content and the ^{129}Xe NMR chemical shift extrapolated to zero xenon coverage of xenon adsorbed in that zeolite. Using this relationship, the chemical shift extrapolated to zero xenon coverage of the treated samples was used to calculate the apparent aluminum content of the zeolite

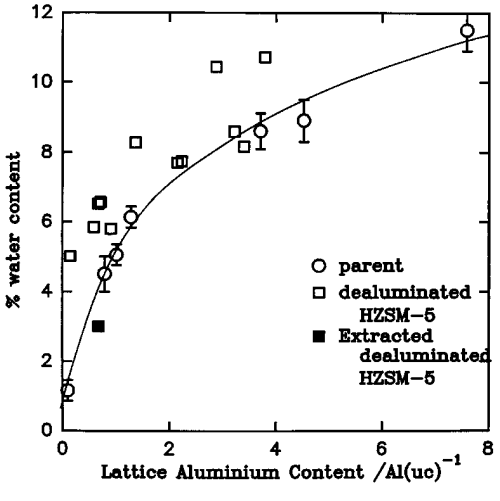

FIG. 7. Water content as a function of lattice aluminum content for HZSM-5 samples.

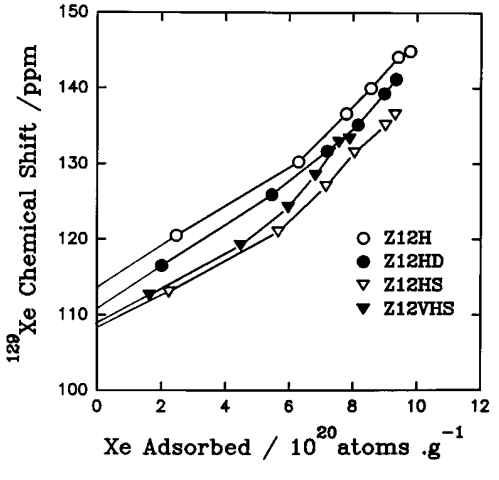

FIG. 8. ^{129}Xe NMR chemical shifts for treated HZSM-5 samples as a function of xenon adsorbed in the zeolite.

lattice. These apparent aluminum contents are given in Table 3.

DISCUSSION

Loss of Lattice Aluminum

Treatment of the zeolite, whether dry heating or steaming, led to a loss of ^{27}Al NMR signal intensity (Fig. 1), despite the finding that the aluminum content of the zeolite, as measured by chemical analysis, had remained unchanged. A similar decrease in total ^{27}Al NMR signal, or formation of NMR invisible aluminum, was observed in previous studies of steam treatment of HZSM-5 (3, 5, 9). Loss of signal can be attributed to the quadrupolar nature of the ^{27}Al nucleus. In a low symmetry environment the second-order interaction between the asymmetrical electric field gradient at the nucleus and the quadrupole moment broadens the NMR signal beyond detection in a simple MAS experiment at the frequency used here. Therefore, following calcination or hydrothermal treatment, the tetrahedral symmetry of the lattice aluminum must be lost and aluminum species of lower symmetry formed. The more severe the treatment, i.e., longer duration or higher temperature, the greater the loss of total NMR visible aluminum. From these ^{27}Al NMR studies it was not possible to determine whether this change in symmetry was due to partial or total removal of aluminum from the zeolite lattice or merely a change in the lattice aluminum environment.

Following deammonation of the HZSM-5 sample a signal of small intensity appeared at −2 ppm. This band is attributed to aluminum with octahedral symmetry (22, 23) and presumably arises from aluminum removed from the zeolite lattice during deammonation treatment. Upon further calcination or hydrothermal treatment, the intensity of this octahedral signal remained the same or decreased, suggesting that while the most easily removed aluminum in the lattice formed octahedral monatomic species, further treatment led to formation of alternative aluminum species of low symmetry.

A broad NMR signal, centered ca. 30–40 ppm, was observed in spectra of the more severely treated samples. A similar signal was reported in studies of dealuminated Y zeolite (24–26) and dealuminated HZSM-5 (6, 7, 9). This signal can be attributed to aluminum in a distorted tetrahedral environment, although the possibility of 5-coordinate aluminum (11) cannot be totally dismissed. Quantification of the broad peak was not attempted.

Loss of signal intensity for the Si(1Al) signal was clearly observed in the ^{29}Si NMR spectra (Fig. 3) following treatment of the zeolite samples and indicates that Si–O–Al bonds in the zeolite lattice are breaking. The aluminum perturbed by the treatment of the zeolite is thus being removed from the zeolite lattice. A narrowing of the Si(0Al) signal and the changes in its profile are also indicative of loss of aluminum from the lattice; resolution of the Si(0Al) signals from crystallographically distinct sites becomes possible if ZSM-5 is completely dealuminated (5).

Further evidence that the loss of ^{27}Al NMR intensity can be attributed to dealumination of the zeolite lattice was found in the infrared measurements of the zeolite framework vibrations. The relationship between the frequencies of the framework vibrational modes and the aluminum content of the zeolite can be seen from the results for the parent HZSM-5 shown plotted in Fig. 6. (Note that this is not linear, in contrast to the analogous relationship reported by Sohn *et al.* (27) for Y zeolite.)

Also shown on these plots are the corresponding framework frequencies for treated HZSM-5 in the Z12 series, plotted as a function of the tetrahedral lattice aluminum as measured by ^{27}Al NMR. The wavenumber of the vibrations in treated samples fell on the line observed for parent HZSM-5 in these plots. The aluminum not observed in the ^{27}Al NMR spectra appears to have been removed from the HZSM-5 lattice as far as the framework vibrational modes are concerned.

The ^{29}Si NMR spectra recorded employing cross-polarization indicate that the concentration of silanol groups was not increased by the calcination or hydrothermal treatments employed. Any defects formed by the removal of lattice aluminum must be healed during heat or steam treatment, as occurs during dealumination of zeolite Y (14, 15). Maijanen *et al.* found that SiOH defects formed in ZSM-5 at short steaming times were removed on prolonged steaming (9). The narrowing of the infrared absorption bands due to framework vibrational modes following treatment indicates a greater degree of ordering or lower defect concentration in the zeolite lattice of these treated samples, and the intensity of the silanol infrared band at 3720 cm^{-1} is observed to decrease following vigorous hydrothermal treatment.

Comparison of the Z12HD and Z12HS HZSM-5 ^{27}Al NMR spectra indicated that although both treatments led to loss of intensity of the tetrahedral lattice signal and formation of aluminum species of low symmetry, the effect of treatment under dry conditions was less severe than under steaming conditions. Datka and Tuznik (1) observed that the calcination carried out in their study caused no dealumination, while steam treatment led to loss of intensity of the tetrahedral aluminum signal in the ^{27}Al NMR spectra.

Loss of aluminum from the zeolite lattice causes loss of the infrared band at 3606 cm^{-1} due to bridging hydroxyl groups, and loss of the band at 1543 cm^{-1} following pyridine adsorption attributed to pyridine adsorbed on Brønsted acid sties. A good correlation existed between the bridging hydroxyl group concentration, the Brønsted acid site concentration, and the lattice aluminum content of treated zeolites. The same observations were made following treatment regardless of the aluminum content of the parent HZSM-5

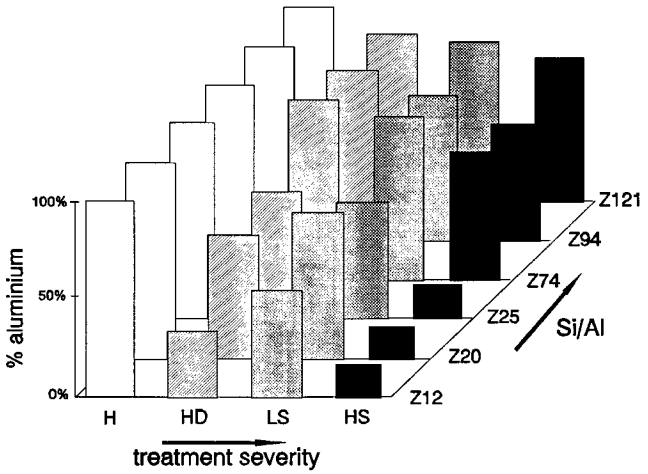

FIG. 9. Schematic representation of the aluminum remaining in the zeolite lattice following calcination and hydrothermal treatment for HZSM-5 samples of differing aluminum content.

sample. Figure 9 represents schematically the aluminum remaining within the zeolite lattice as a function of both the severity of the treatment and the Si/Al ratio of the parent zeolite. For a given treatment the extent of dealumination decreased with decreasing aluminum content of the parent HZSM-5; i.e., HZSM-5 of low aluminum content was more resistant to dealumination than were samples of higher aluminum content.

Extralattice Aluminum

It is clear that both calcination and hydrothermal treatment of HZSM-5 removed considerable quantities of aluminum from the zeolite lattice. Chemical analysis revealed that this aluminum, called hereafter extralattice aluminum, remained in the zeolite sample. The NMR invisibility of the majority of this extralattice aluminum indicated that the aluminum is in sites of less than cubic symmetry, with the exception of a small portion of the extralattice aluminum represented in the ^{27}Al NMR spectra by the signal at ca. 0 ppm and assigned to octahedral extralattice aluminum.

Presence of this extralattice aluminum in the treated samples was demonstrated by the use of acetylacetone adsorption. We have shown previously (16) that acetylacetone adsorption cannot be relied upon to yield quantitative information on the extralattice aluminum content but is, however, capable of providing diagnostic information on the presence of extralattice aluminum. Appearance of a sharp ^{27}Al signal attributed to octahedral aluminum in the ^{27}Al NMR spectra of treated HZSM-5 samples on which acetylacetone had been adsorbed (Fig. 2) confirmed the presence of extralattice aluminum.

The infrared absorption observed at ca. 3660 cm^{-1} in the infrared spectra of mildly treated Z12 is attributed to hydroxyl groups associated with extralattice aluminum species and was the same as a band observed previously (9) in mildly steamed HZSM-5. This band was not observed in the most severely steamed samples (Fig. 4e). A similar band is reported in the literature at 3600 cm^{-1} in the spectra of dealuminated Y zeolites (28). Patzelova *et al.* (29) noted that strong dealumination of Y zeolite led to the loss of the band associated with extralattice aluminum. This loss was attributed to the condensation of low-molecular-weight extralattice aluminum species formed under mild dealumination conditions, into polymeric aluminum species under more vigorous treatment and loss of the accompanying hydroxyl groups. We believe that the same explanation can be used here to account for our observations and those of Maijanen *et al.* (9) on HZSM-5.

Infrared spectra of pyridine adsorbed on HZSM-5 samples allowed also the Lewis acidity to be studied. The intensity of the IR band at 1454 cm^{-1} observed for Z12 HZSM-5 which had been deammonated carefully in the FTIR cell (denoted Z12NH) corresponded to ca. 2% of the total acid site concentration and was attributed to coordination of pyridine on residual sodium cations in the zeolite.

Deammonation treatment to prepare the Z12H sample led to a significant increase in Lewis acid site concentration. The Lewis site concentration increased to a small extent on further mild treatment of the zeolite, but decreased again on strong steam treatment. The Lewis acid site concentration of the Z12VHS sample was only marginally higher than can be explained by residual sodium ions. There was no direct correlation observed between the concentration of Lewis acid sites and the extralattice aluminum content of the treated zeolite. We note that under our conditions the infrared band at 1440 cm^{-1} attributed by Maijanen *et al.* (9) to pyridine adsorbed on weak Lewis acid sites was not observed.

The same total acid concentration was measured by adsorption of the smaller ammonia molecule; i.e., the low Lewis acid site concentrations measured with pyridine are not due to steric restrictions. Extraction of extralattice aluminum with hexafluorosilicate decreased the Lewis acid site concentration.

The mass of water adsorbed in the HZSM-5 samples was greater in all cases for dealuminated zeolites containing extra lattice aluminum than would be expected from the lattice aluminum content. This was true both for samples containing octahedral aluminum species (Z12HD, Z12HS) and samples for which the ^{27}Al NMR spectra showed no evidence of extralattice aluminum of octahedral symmetry (Z20HS). The greater the extralattice aluminum content of the zeolite sample, the greater the difference between the measured water content and that expected from the lattice aluminum content of the sample. In addition, extraction of the extralattice aluminum gave a sample (Z20S/SW) with water content identical to that expected from the lattice aluminum content. Extralattice aluminum species

evidently provide additional sites for adsorption of water in the zeolite.

Upon dealumination the pore volume of the zeolite decreased. X-ray diffraction and ^{29}Si NMR indicated that this was not due to loss of crystallinity of the zeolite. Thus we attribute the decreased pore volume to extralattice aluminum occupying volume in the channel system; the pore volume loss increased with increasing content of extralattice aluminum. Extraction of the extralattice aluminum partially restored the lost pore volume (Table 3). Surface analysis by XPS indicates some enhancement of aluminum at the crystal surface, suggesting that migration of the extralattice aluminum through the zeolite pores does occur during more severe hydrothermal treatment.

The gradients of ^{129}Xe NMR chemical shift versus xenon coverage plots depend on the zeolite micropore volume, since this determines the effective xenon density in the sample (30). Negligible changes in the gradients of these plots were observed here for treated samples; however, as shown by Ito *et al.* (31) for ZSM-5 containing coke deposits, the method is insensitive to small pore volume changes. The chemical shift extrapolated to zero xenon coverage does decrease significantly as a result of treatment of the zeolite (Fig. 8). It is known (18) that the chemical shift at zero xenon coverage depends on the aluminum content of the lattice, which determines the average electrostatic field experienced by the xenon. Dealumination of the zeolite lattice should therefore decrease the xenon chemical shift. However, the apparent aluminum content of the zeolite lattice calculated from the chemical shift at zero xenon coverage was consistently higher than the value of lattice aluminum content found from ^{27}Al NMR or FTIR; it was only for samples where the extralattice aluminum content was low (Z20HD, Z25HD) that the lattice aluminum contents measured by both methods were the same within experimental error. We attribute this difference to extralattice aluminum remaining in the zeolite pores and contributing to the average electric field experienced by xenon.

A number of differences are noted between the dealumination of HZSM-5 and HY zeolites. Though in both cases the degree of dealumination is a function of the same set of factors such as the water vapor pressure of the treatment (7, 14) or treatment temperature (15), the species of extralattice aluminum subsequently formed apparently differ.

Hydrothermal dealumination of HY leads to large concentrations of octahedral aluminum (15) and in sharp contrast to results in this study the major portion of the extralattice aluminum remains NMR visible. Infrared spectra of dealuminated HY also indicate higher proportions of hydroxyl groups attached to extralattice aluminum (29) and considerably greater Lewis acid site concentrations (32) than observed here for dealuminated HZSM-5.

The extralattice aluminum species formed initially in dealuminated HY zeolites are postulated to be the monomeric aluminum-oxo-hydroxides (33) and a body of evidence exists in the literature (28a, 29, 34) indicating that condensation to polymeric aluminum species such as pseudoboemhite (35) occurs as a result of the more severe treatment. Clearly the final extralattice aluminum product formed following dealumination of HZSM-5 is not the same as that in HY. However, as the mechanism of dealumination appears to be very similar we suggest that the initial aluminum species may well be the same for both zeolites and that it is the different pore sizes of the zeolites which influence the extent of the migration and/or polymerization of extralattice aluminum species.

ACKNOWLEDGMENT

Financial support from Chemistry Division, Department of Scientific and Industrial Research, New Zealand (now known as Industrial Research Ltd) is gratefully acknowledged.

REFERENCES

1. Datka J., and Tuznik, E., *J. Catal.* **102**, 43 (1986).
2. Jacobs, P. A., Tielen, M., Nagy, J. B., Debras, G., Derouane, E. G., and Gabelica, Z., *in* "Proceedings, 6th International Zeolite Conference" (D. Olson and A. Bisio, Eds.) p. 783. Butterworths, Stoneham, MA, 1984.
3. Klinowski, J., Thomas, J. M., Fyfe, C. A., and Gobbi, G. C., *Nature* **296**, 533 (1982).
4. Freude, D., Brunner, E., Pfeifer, H., Prager, D., Jerschkewitz, H.-G., Lohse, U., and Oehlmann, G., *Chem. Phys. Lett.* **139**, 325 (1987).
5. Fyfe, C. A., Gobbi, G. C., and Kennedy, G. J., *J. Phys. Chem.* **88**, 3248 (1984).
6. Bosacek, V., Freude, D., Frohlich, T., Pfeifer, H., and Schniedel, H., *J. Coll. Interface Sci.* **85**, 502 (1982).
7. Brunner, E., Ernst, H., Freude, D., Frohlich, T., Hunger, M., and Pfeifer, H., *J. Catal.* **127**, 34 (1991).
8. Samoson, A., Lippmaa, E., Engelhardt, G., Lohse, U., and Jerschkewitz, H. G., *Chem. Phys. Lett.* **134**, 589 (1987).
9. Maijanen, A., Derouane, E. G., and Nagy, J. B., *Appl. Surf. Sci.* **75**, 204 (1994).
10. Lago, R. M., Haag, W. O., Mitovsky, R. J., Olson, D. H., Hellring, S. D., Schmitt, K. D., and Kerr, G. T., *in* "Studies in Surface Science and Catalysis" (Murakima, Ed.), Vol. 28, p. 677 (1986).
11. Coster, D., and Fripiat, J. J., *Chem. Mater.* **5**, 1204 (1993).
12. Topsoe, N. Y., Pedersen, K., and Derouane, E. G., *J. Catal.* **70**, 41 (1981).
13. Engelhardt, G., Lohse, U., Samoson, A., Magi, M., Tarmak, M., and Lippmaa, E., *Zeolites* **2**, 59 (1982).
14. Engelhardt, G., Lohse, U., Patzelova, V., Magi, M., and Lippmaa, E., *Zeolites* **3**, 233 (1983).
15. Freude, D., Frohlich, T., Pfeifer, H., and Scheler, G., *Zeolites* **3**, 171 (1983).
16. Alexander, S. M., Bibby, D. M., Howe, R. F., and Meinhold, R. H., *Zeolites* **13**, 441 (1993).
17. Moon, S. H., Windawi, H., and Katzer, J. R., *Ind. Eng. Chem. Fund.* **20**, 396 (1981).
18. Alexandar, S. M., Coddington, J. M., and Howe, R. F., *Zeolites* **11**, 368 (1991).
19. Datka, J., *J. Chem. Soc. Faraday Trans.* **77**, 2877 (1981).
20. Tallon, J. L., and Buckley, R. G., *J. Phys. Chem.* **91**, 1469 (1987).
21. Defosse, C., Delmon, B., and Canesson, P., *ACS Symp. Ser.* **40**, 86 (1977).

22. Muller, D., Gessner, W., Behren, H. J., and Scheler, G., *Chem. Phys. Lett.* **79**, 59 (1981).
23. Bosacek, V., and Freude, D., *in* "Innovations in Zeolite Materials Science" (P. J. Grobet *et al.*, Eds), p. 231. Elsevier, Amsterdam, 1988.
24. Klinowski, J., Fyfe, C. A., and Gobbi, G. C., *J. Chem. Soc. Faraday Trans. I*, **81**, 3003 (1985).
25. Lippmaa, E., Samoson, A., and Magi, M., *J. Am. Chem. Soc.* **108**, 1730 (1986).
26. Gilson, J. P., Edwards, G. G., Peters, A. W., Rajagopalan, K., Wormsbecher, R. F., Roberie, T. G., and Shatlock, M. P., *J. Chem. Soc. Commun.* **91**, (1987).
27. Sohn, J. R., DeCanio, S. J., Lunsford, J. H., and O'Donnell, D. J., *Zeolites* **6**, 225 (1986).
28. (a) Jacobs, P. A., and Uytterhoeven, J. B., *J. Chem. Soc. Faraday Trans.* **69**, 373 (1973); (b) Jacobs, P. A., and Uytterhoeven, J. B., *J. Catal.* **22**, 193 (1971); (c) Scherzer, J., and Bass, J. L., *J. Catal.* **28**, 101 (1973); (d) Anderson, M. W., and Klinowski, J., *Zeolites* **6**, 455 (1986); (e) Fritz, P. O., and Lunsford, J. H., *J. Catal.* **118**, 85 (1989).
29. Patzelova, V., Drahoradova, E., Tvaruzkova, Z., and Lohse, U., *Zeolites*, **9**, 74 (1989).
30. Johnson, D. W., and Griffiths, L., *Zeolites* **7**, 484 (1987).
31. Ito, T., Bornardet, J. E., Fraissard, J., Nagy, J. B., Andre, C., Gabelica, Z., and Derouane, E. G., *Appl. Catal.* **43,**, L5 (1988).
32. Ward, J. W., *J. Catal.* **9**, 225 (1967).
33. Brunner, E., Ernst, H., Freude, D., Hunger, M., and Pfeifer, H., *in* "Innovations in Zeolite Materials Science" (P. J. Grobet *et al.*, Eds.), p. 155. Elsevier, Amsterdam, 1985.
34. (a) Vedrine, J. C., Abou-Kais, A., Massardier, J., and Dolmai-Imelik, G., *J. Catal.* **29**, 120 (1973). (b) Lohse, U., Loffler, E., Hunger, M., Stockner, J., and Patzelova, V., *Zeolites* **7**, 11 (1987).
35. Shannon, R. D., Gardner, K. H., Stadey, R. H., Bergeret, G., Gallezot, P., and Auroux, A., *J. Phys. Chem.* **89**, 4778 (1985).